JOURNAL OF OCULAR PHARMACOLOGY AND THERAPEUTICS
Volume 39, Number 5, 2023

DOI: 10.1089/jop.2022.0187

Open camera or QR reader and scan code to access this article and other resources online.

Dietary Alcohol Consumption Elicits Corneal Toxicity Through the Generation of Cellular Oxidative Stress

Anita K. Ghosh,[1,2] Robertas Čėsna,[3,4] Donatas Neverauskas,[3,4] Agnė Žiniauskaitė,[3,4] Sana Iqbal,[5–7] Jonathan M. Eby,[1] Symantas Ragauskas,[3] and Simon Kaja[2,6,7]

Abstract

Purpose: Clinical data suggest that alcohol use is associated with the development of signs and symptoms of dry eye disease. However, preclinical data investigating ocular toxicity after dietary alcohol consumption are lacking. In this study, we investigated the effects of alcohol on the ocular surface, in human corneal epithelial cells (HCE-T) *in vitro* and in C57BL/6JRj mice *in vivo*.
Methods: HCE-T were exposed to clinically relevant doses of ethanol. To determine the effects of dietary alcohol consumption *in vivo*, wild-type mice were administered the Lieber–DeCarli liquid diet (5% vol/vol ethanol or isocaloric control) for 10 days *ad libitum*. Corneal fluorescein staining was performed to assess ocular surface damage. Histopathological and gene expression studies were performed on cornea and lacrimal gland tissue.
Results: Sublethal doses of ethanol (0.01%–0.5%) resulted in a dose-dependent increase of cellular oxidative stress in corneal epithelial cells and a significant increase in *NFE2L2* and downstream antioxidant gene expression, as well as an increase in NFκB signaling; short-term exposure (0.5%, 4 h) triggered significant corneal epithelial cell barrier breakdown. Exposure to the alcohol-containing diet caused a 3-fold increase in corneal fluorescein staining, with no effect on tear volumes. Corneal thickness was significantly reduced in the alcohol diet group, and corneal tissue revealed dysregulated antioxidant and NFκB signaling. Our data provide the first published evidence that alcohol exposure causes ocular toxicity in mice.
Conclusions: Our results are consistent with clinical studies linking past alcohol consumption to signs of ocular surface disease.

Keywords: alcohol, ocular surface disease, dry eye, conjunctivitis, cornea, oxidative stress

Introduction

Dry eye disease (DED) is a debilitating multifactorial disease with subtypes differentially affecting components of the ocular surface. In patients, DED manifests as ocular pain or discomfort, blurry vision, grittiness, and light sensitivity as a result of tear film dyshomeostasis.[1] While age and gender are the strongest risk factors, environmental, pharmaceutical, and genetic factors are important etiological contributors.

[1]Graduate Program in Biochemistry and Molecular Biology, Health Sciences Division, Loyola University Chicago, Maywood, Illinois, USA.
[2]Research & Development Division, Experimentica Ltd., Forest Park, Illinois, USA.
[3]Research & Development Division, Experimentica Ltd., Vilnius, Lithuania.
[4]State Research Institute Centre for Innovative Medicine, Vilnius, Lithuania.
[5]Graduate Program in Molecular Pharmacology and Therapeutics, Health Sciences Division, Loyola University Chicago, Maywood, Illinois, USA.
Departments of [6]Ophthalmology and [7]Molecular Pharmacology & Therapeutics, Stritch School of Medicine, Loyola University Chicago, Maywood, Illinois, USA.

Clinical evidence suggests that both acute and chronic alcohol use are associated with the development of signs and symptoms of DED. Most notably, the longitudinal 15-year population-based Beaver Dam Study reported that DED symptoms were positively associated with a history of alcohol consumption.[2] In a comparative case–control study of heavy male drinkers (≥4 drinks per day) and age-matched healthy nondrinkers, alcohol consumption was associated with a decreased tear breakup time, lower tear volumes, and abnormal conjunctival impression cytology.[3] These data suggest a tentative association between chronic alcohol abuse and prevalence/risk of DED.

A separate case–control study revealed that healthy male volunteers who consumed a single dose of alcohol (0.75 g ethanol per kg body weight) exhibited higher tear osmolarity, faster tear breakup time, and higher fluorescein scores within just 12 h of alcohol consumption.[4] Notably, alcohol tissue levels were ~50% of plasma levels, providing a rationale for alcohol eliciting local toxicity on tissues of the ocular surface. However, despite clinical evidence, to our knowledge there are no published studies investigating the effects of dietary alcohol exposure on the ocular surface *in vivo*. Similarly, mechanistic *in vitro* studies investigating sublethal doses of ethanol are missing.

Alcohol is well known to elicit tissue and organ damage through generation of reactive oxygen species (ROS). While many of the detailed tissue-specific mechanisms of ethanol toxicity and the involvement of oxidative stress pathways are not yet fully elucidated, ethanol metabolism has been associated with increased levels of oxidative stress through alcohol dehydrogenase, the microsomal ethanol oxidation system, and catalase (CAT) metabolic pathways.[5,6] We thus hypothesized that alcohol could result in oxidative stress-mediated ocular toxicity. Therefore, the purpose of this study was to elucidate the effects of ethanol on human corneal epithelial cells (HCE-T) *in vitro* and of dietary alcohol exposure in C57BL/6JRj mice *in vivo*. To our knowledge, this is the first study to rigorously investigate the effects of alcohol on the ocular surface in preclinical models.

Our data show that alcohol elicits deleterious effects on the tissues of the ocular surface and identify the generation of cellular oxidative stress as the likely underlying mechanism of alcohol-induced ocular surface damage. Our results warrant future preclinical and clinical studies assessing the association between alcohol consumption and ocular surface disease.

Methods

Cell culture

HCE-T[7] were obtained from RIKEN Research Institute (Tokyo, Japan) and cultured according to the provider's instructions. Specifically, HCE-T were maintained in Dulbecco's modified Eagle's medium (DMEM)/F12 (1:1; Thermo Fisher Scientific, Waltham, MA) with 5% fetal bovine serum (Gemini Bio Products, West Sacramento, CA), 0.5% dimethyl sulfoxide, 5 μg/mL insulin (both from Millipore Sigma), 10 ng/mL human recombinant epidermal growth factor, and 100 U/mL penicillin–100 mg/mL streptomycin (both from Thermo Fisher Scientific) and grown in tissue culture flasks (Techno Plastic Products, MidSci, St. Louis, MO). Cultures of passages 79–98 were used for experiments.

Cell viability assays

3-(4,5-Dimethylthiazol-2-yl)-2,5-diphenyltetrazolium bromide (MTT) and lactate dehydrogenase (LDH) release assays were conducted essentially as described by us for other ocular cell types.[8–10]

Quantification of generation of ROS

ROS generation was quantified using the general oxidative stress indicator, chloromethyl 2′,7′-dichlorodihydrofluorescein diacetate (CM-H_2DCFDA; Thermo Fisher Scientific), as per the manufacturer's instructions. Cells were seeded at a density of 10,000 cells/well in white side, clear bottom 96-well plates (Greiner Bio-One, Monroe, NC). When reaching confluency (48 h), cells were loaded with 5 μM of CM-H_2DCFDA in phenol red-free complete media for 30 min. Reagent was aspirated, before treating cells with experimental conditions, that is, phenol red-free complete media supplemented with either tert-butyl hydroperoxide (*t*BHP) or ethanol for the time desired. Fluorescence was measured (excitation: 492, emission: 520, gain: 1,000) using a FLUOstar OPTIMA plate reader (BMG LABTECH, Ortenberg, Germany).

Cellular permeability assays

Cells were seeded at a density of 100,000 cells/well in 12 mm Transwell® with 0.4 μm pore polycarbonate membrane inserts (Corning, Inc., Corning, NY). Cells were maintained in complete media for the duration of the experiment; the assay was performed in complete media without phenol red. Cells were stratified on the inserts as described previously.[11] Briefly, cells were maintained for 1 week in complete media (0.5 mL media in the donor chamber, 1.5 mL media in the receiver chamber) before stratification in a liquid air interface for 3 weeks (1 mL media in the receiver chamber only). Media was replenished every other day throughout the experiment.

Stratified cells were treated with 5 μM *t*BHP or 0.5% ethanol in complete media for 4 h; control cells were maintained in complete media. To quantify permeability across HCE-T, complete media was replaced with phenol red-free media supplemented with the fluorescent indicators, 6-carboxyfluorescein (6-CF; 100 μM) and Rhodamine B (RhoB; 50 μM). Samples were removed from the donor (10 μL) and receiver (100 μL) chambers at 0, 30, 50, 70, 90, 120, 150, and 180 min. Sample volume removed was replaced by complete media and accounted for in the calculations.

Standard curves for 6-CF and RhoB were prepared in complete media using 0, 10, 20, 30, 40, and 50 μM RhoB and 0, 20, 40, 60, 80, and 100 μM 6-CF, respectively.

Fluorescence was measured using a Cytation 5 imaging plate reader (Biotek, Winooski, VT; RhoB- excitation: 553 nm, emission: 627 nm; 6-CF- excitation: 490 nm, emission: 520 nm). The absolute amount (in moles) of the fluorescent permeability standards present in donor and receiver chambers at each time point was calculated using the standard curve, taking into account the volume removed and replaced with media in the final calculations. The apparent permeability index (P_{app}) was calculated as described previously.[11]

Immunocytochemistry

HCE-T were seeded at a density of 100,000 cells/mL on 8-well chamber slides (Thermo Fisher Scientific). Once

confluent, cells were treated with ethanol or *t*BHP for 6 h, then fixed with 4% PFA for 15 min. Immunocytochemistry was performed as described previously[12,13] using mouse anti-ZO1 antibody (Cat. No. 339100, dilution 1:250; Thermo Fisher Scientific) and rabbit anti-occludin (Cat. No. 71-1500, 1:250; Thermo Fisher Scientific). Immunoreactivity was quantified by fluorimetry using Fiji software.[14]

Quantification of epithelial cell barrier function

Tight junction organization rate (TiJOR) as a quantitative parameter for barrier function and tight junction strength was quantified essentially as originally described by Ref.[15] Specifically, 3 rectangles increasing in size were drawn per image using FIJI (ImageJ; NIH, Bethesda, MD), and the number of ''junctions'' or lines that the rectangle crossed was counted manually by a blinded investigator. The number of lines was divided by the perimeter of the rectangle, to yield the TiJOR ratio value.

Protein extraction and western blot

Total protein was extracted from HCE-T using the NE-PER Nuclear and Cytoplasmic Extraction Kit (Thermo Fisher Scientific). Invitrogen™ Bolt™ 4%–12% Bis-Tris protein gels (Thermo Fisher Scientific) were loaded with 5 µg of nuclear protein lysate and run at 100 V for 22 min. Dry transfer was performed in an iBlot2™ system (Thermo Fisher Scientific) at 12 V for 12 min, using prepackaged transfer stacks, according to the manufacturer's instructions. Washes and antibody incubations were performed in an iBind™ Flex western device (Thermo Fisher Scientific), using commercially available reagents according to the manufacturer's instructions, an anti-RELA antibody (mouse anti-RELA, Cat. No. MAB5078, 1:100 dilution, vendor), and HRP-linked secondary antibodies (1:4,000; Cytiva Life Sciences, Marlborough, MA). Blots were developed with SuperSignal™ West Femto substrate (Thermo Fisher Scientific) and imaged using a ChemiDoc™ XRS+ System (Bio-Rad Laboratories, Hercules, CA).

Relative protein expression was quantified by densitometry of bands using Image Lab software (Bio-Rad Laboratories) and data normalized to lamin B1 (rabbit anti-lamin B1, Cat. No. 16048, dilution 1:2,000; Abcam) and the control condition.

Quantification of cytokine release

HCE-T were seeded at a density of 150,000 cells/well in 6-well plates. Once confluent, cells were exposed to ethanol at indicated doses for 6 h. Media samples were collected and stored at −80°C. Samples were sent for analysis using a commercially available Human Cytokine/Chemokine 48-Plex Discovery Assay® Array (HD48; Eve Technologies, Calgary, Canada).

Transepithelial electrical resistance measurements

Transepithelial electrical resistance (TEER) measurements were performed in stratified HCE-T (as described above) using an EVOM2 handheld volt meter (World Precision Instruments, Sarasota, FL).

Animals

All animals were treated in accordance with the ARVO Statement for the Use of Animals in Ophthalmic and Vision Research and the European Commission Directive 86/609/EEC for animal experiments, using protocols approved and monitored by the State Veterinary Agency of Lithuania (protocol number G2-151, approved 9/5/2020). C57BL/6JRj mice were purchased from Janvier Labs (Le Genest-Sainte-Isle, France). Mice were housed at a constant temperature (22°C ± 1°C) and in a light-controlled environment (lights on from 7 a.m. to 7 p.m.) with *ad libitum* access to food and water. Male mice (12 weeks of age) were used for experiments.

All procedures (tear volume measurements, corneal fluorescein staining, and euthanasia) were performed after inducing a deep plane of general anesthesia by intraperitoneal administration of a cocktail of 50 mg/kg ketamine and 10 mg/kg medetomidine.

For experiments, all mice were acclimated to the rodent Lieber–DeCarli liquid diet (BioServ®, Flemington, NJ) for 3 days. Thereafter, mice either continued to receive the rodent Lieber–DeCarli liquid diet or were switched to an alcohol-containing diet (BioServ) with 5% alcohol. Both diets had the same caloric content and were prepared according to Ref.[16]

Tear volume measurements

Tear volume quantification was performed by applying a sterile phenol red-soaked cotton thread (ZoneQuick™; Showa Yakuhin Kako Co. Ltd., Tokyo, Japan) into the lateral canthus for 10 s. The wetting length of the thread was read under a microscope using a ruler. Resolution of the measurements was 0.5 mm. Tear volume was measured in all groups, at baseline and at the end of the 10-day study period.

Corneal fluorescein staining

To quantify ocular surface damage, we scored corneal fluorescein staining, essentially as described by us previously[11,17] using I-Dew Flo Fluorescein Sodium ophthalmic strips (OptiTech Eyecare, Prayagraj, India) under systemic anesthesia. The cornea was imaged using a fluorescent microscope (Leica Microsystems, Wetzlar Germany). In addition, images were acquired using a Spectralis® HRA+OCT (Heidelberg Engineering, Heidelberg, Germany).

Tissue collection and histology

Mice were euthanized by cervical dislocation while under a deep surgical plane of anesthesia. Whole eyes, including ocular surface tissues, were dissected and embedded in optimal cutting temperature compound (Tissue-Tek®; Sakura Finetek USA, Torrance, CA), and frozen sections (10 µm) were prepared using a cryostat (Leica Microsystems).

Extraorbital lacrimal glands were dissected, embedded in paraffin, and sectioned (5 µm). Tissue sections were processed for histological analysis using hematoxylin-eosin staining.[18] Corneal thickness was quantified using ImageJ software (NIH).

Total RNA isolation, complementary DNA synthesis, and quantitative polymerase chain reaction

HCE-T or frozen tissue (cornea, extraorbital lacrimal glands) was harvested and homogenized directly in lysis buffer, and total RNA was isolated using the Total RNA Purification Plus Kit (Norgen Biotek, Ontario, Canada), as per the manufacturer's instructions. Genomic DNA (gDNA) was removed using gDNA removal columns (Norgen Biotek). RNA quality and concentration were assessed using a nanospectrophotometer (Nanodrop; Thermo Fisher Scientific). Complementary DNA (cDNA) synthesis was performed using the High Capacity cDNA reverse transcription Kit (Thermo Fisher Scientific) with 1 μg cDNA per 20 μL reaction.

Quantitative polymerase chain reaction (qPCR) was performed in reverse transcriptase (RT)-PCR reactions (15 μL volume) containing 7.5 μL TaqMan® Fast Gene Expression Master Mix, 0.75 μL TaqMan Gene Expression Assay, 10 ng cDNA template, and water. Reactions were performed in triplicates. RT-PCR amplification was performed on 96-well PCR microplate (Thermo Fisher Scientific) in an AriaMX Real-Time PCR system (Agilent, Santa Clara, CA). Relative expression was quantified using the $2^{-\Delta\Delta CT}$ method as previously described,[19] with GAPDH as endogenous control. TaqMan Gene Expression Assay ID numbers are provided in Supplementary Table S1.

Statistical analysis

Experimental group sizes were determined by *a priori* power analyses based on previous studies (including Ref.[8,11,18,20]) and the published literature using G*Power software.[21,22] For cytokine analysis, a group size of $n=3$ was calculated to detect a >20% change with an α of 0.05 and a power of 95%, corresponding to an effect size of 4.1. Based on our previous experiments investigating barrier function, we determined a sample size of $n=3$ per group to detect a >5% change with an α of 0.05 and a power of 95%, corresponding to an effect size of 5.93. For *in vivo* studies, we extrapolated an estimated group size of $n=10$ from our published data in the mouse desiccating stress/scopolamine (DSS) model with a power of 90% and an α of 0.05 to detect a 1 score change in the median score of corneal fluorescein staining using the modified Oxford score using a 2-tailed, unpaired Mann–Whitney ranks test.

Power analysis for NF-κB gene expression analysis was based on an *a priori* calculation using standard deviations from previous experiments and the goal to detect a change of >25%, which resulted in an effect size of 2.5 (for a 2-tailed, unpaired *t*-test, an alpha probability of 0.05 and a power of 95%), yielding a required sample size of $n=6$ per group. For quantification of genes involved on redox homeostasis we designed experiments to detect a change of >20%, which resulted in an effect size of 3.63, yielding a required sample size of $n=4$ per group.

Data were graphed and statistically analyzed using Prism 9 software (GraphPad, Inc., La Jolla, CA). Statistical significance was defined as $P<0.05$. Data were analyzed using Student's *t*-test or Mann–Whitney test when comparing 2 groups. For data sets with multiple variables, 2-way analysis of variance (ANOVA) was performed, with treatment (ethanol/alcohol vs. vehicle/control) and time as independent variables. Multiple comparisons tests were performed if ANOVA revealed a statistically significant effect on the independent variables or the interaction. Data are presented showing individual datapoints, with each data point representative of a single biological replicate (n).

Results

Sublethal doses of ethanol elicit significant induction of cellular oxidative stress and upregulation of antioxidant enzymes

To determine the acute cytotoxicity of ethanol, the effects of increasing ethanol concentrations on HCE-T cell viability were tested by MTT and LDH release assays. HCE-T were exposed to a dose–response of ethanol (0.01%–10%) in complete media for 48 h. LDH assay did not show elevated LDH release up to 1% ethanol, while 5% elicited a significant 24% ± 10% increase in LDH release, suggestive of cytotoxicity at this dose (Fig. 1A). MTT assay did not reveal any significant changes in cell proliferation and/or viability (Fig. 1B).

Ethanol is a well-known inducer of cellular oxidative stress; therefore, HCE-T were loaded with 5 μM CM-H$_2$DCFDA, a general oxidative stress indicator, for 30 min and subsequently incubated with 0.01%, 0.05%, 0.1%, or 0.5% ethanol for 4 h. DCF fluorescence increased significantly, by 306% ± 90%, 296% ± 53%, and 946% ± 144%, respectively (Fig. 1C). Oxidative stress and increased ROS generation are often associated with dysregulation of the enzymes of the endogenous antioxidant system, many of which are directly regulated by the master transcription factor, nuclear factor erythroid 2-related factor 2 (Nrf2), encoded by the *NFE2L2* gene.

To investigate the effect of acute ethanol exposure on the endogenous antioxidant system, HCE-T were treated with 0.5% (85 mM) ethanol in complete media for 2, 4, 6, or 12 h, while control cells were maintained in complete media for the equal amount of time. *NFE2L2* expression was quantified by qPCR. Ethanol exposure for 2, 4, and 6 h resulted in significant 247% ± 18% ($n=4$, $P<0.001$), 233% ± 24% ($n=4$, $P<0.01$), and 213% ± 23% ($n=4$, $P<0.001$) increases in *NFE2L2* expression, respectively; *NFE2L2* expression at 12 h was similar to baseline ($n=3$; $P=0.16$; Fig. 1D). Expression of anti- and pro-oxidant enzymes was quantified after 6 h ethanol exposure. CAT, heme-oxygenase 1, and superoxide dismutases 1 and 2 (SOD1 and SOD2) are Nrf2-activated phase 2 antioxidant enzymes involved in mechanisms of reduction of excess superoxide and peroxide, while NADPH oxidases (NOXs) generate superoxide from the oxidation of NADPH. Ethanol resulted in a significant 28% ± 8% ($n=3$, $P<0.05$) induction of *CAT* (Fig. 1E), 43% ± 13% ($n=3$, $P<0.05$) induction of heme oxygenase-1 (*HO-1*; Fig. 1F), 16% ± 4% ($n=3$, $P<0.05$) induction of *SOD2* (Fig. 1H), and 25% ± 9% ($n=3$, $P<0.05$) reduction of NADPH oxidase 3 (*NOX3*; Fig. 1J) gene expression.

No significant changes were observed for *SOD1* ($n=3$, $P=0.23$; Fig. 1G) or NADPH oxidase 2 (*NOX2*; $n=3$; $P=0.61$; Fig. 1I). Together these data suggest that acute short-term exposure of corneal epithelial cells to sublethal doses of ethanol result in significant dysregulation of the endogenous antioxidant balance as a result of significantly increased cellular levels of oxidative stress.

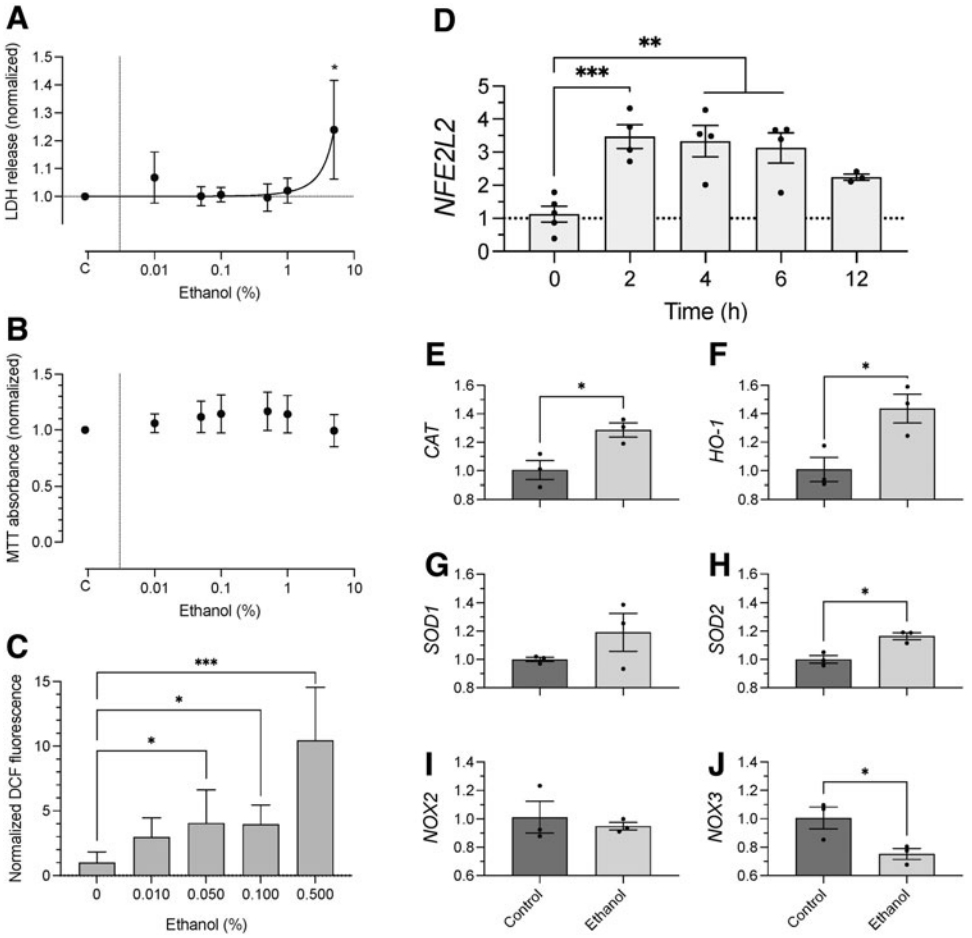

FIG. 1. Sublethal ethanol exposure induces ROS and activates Nrf2-mediated endogenous antioxidant signaling. **(A)** Acute ethanol exposure of concentrations up to 1 μM did not result in increased LDH release from HCE-T. In contrast, 5 μM alcohol caused significant increases in LDH release from HCE-T ($n = 3$). Data are shown as mean ± SEM from 3 separate experiments each derived 8 technical replicates. Data were analyzed by 2-way ANOVA with Dunnett's multiple comparisons test. **(B)** MTT assay revealed no significant cytotoxicity of HCE-T when exposed up to 5% ethanol vol/vol for 48 h ($n = 3$). Data are shown as mean ± SEM from 3 separate experiments each derived 8 technical replicates. Data were analyzed by 2-way ANOVA with Dunnett's multiple comparisons test. **(C)** Ethanol caused a dose-dependent generation of ROS and oxidative stress in HCE-T ($n = 8$). Data are shown from a representative experiment as mean ± SD from 8 replicates. Data were analyzed by 2-way ANOVA with Holm-Šídák multiple comparisons test. **(D)** HCE-T were exposed to 0.5% ethanol for 2, 4, 6, or 12 h, which cause a time-dependent increase in *NFE2L2* mRNA levels that were different to untreated control at 2, 4, and 6 h ($n = 5$). Data are shown as mean ± SEM from 5 separate experiments each derived from 3 technical replicates. Data were analyzed by 2-way ANOVA with Dunnett's multiple comparisons test. **(E–J)** HCE-T were treated with 0.5% ethanol for 6 h, and mRNA levels of **(E)** *CAT*, **(F)** *HO-1*, **(G)** *SOD1*, **(H)** *SOD2*, **(I)** *NOX2*, and **(J)** *NOX3*. Expression levels of *CAT*, *HO-1*, and *SOD2* were significantly increased by ethanol exposure, and NOX3 levels were significantly decreased ($n = 3$–5). qPCR data are shown as mean ± SEM derived from 3 separate experiments with 3 technical replicates each. Data were analyzed by Student's *t*-test. $^{*}P < 0.05$, $^{**}P < 0.01$, $^{***}P < 0.001$. ANOVA, analysis of variance; *CAT*, catalase; HCE-T, human corneal epithelial cells; *HO-1*, heme oxygenase-1; LDH, lactate dehydrogenase; mRNA, messenger RNA; MTT, 3-(4,5-dimethylthiazol-2-yl)-2,5-diphenyltetrazolium bromide; *NOX2*, NADPH oxidase 2; *NOX3*, NADPH oxidase 3; Nrf2, nuclear factor erythroid 2-related factor 2; qPCR, quantitative polymerase chain reaction; ROS, reactive oxygen species; SD, standard deviation; SEM, standard error of the mean; SOD1, superoxide dismutase 1; SOD2, superoxide dismutase 2.

Ethanol activates NF-κB signaling and elicits secretion of pro-angiogenic cytokines in HCE-T

Elevated levels of oxidative stress can activate NF-κB signaling, which can in turn exert cytoprotective effects by suppressing ROS accumulation, but also induce inflammatory signaling pathways. Given the known dysregulation of NF-κB signaling in DED, expression of the canonical signaling proteins NFKB1 (P50) and RELA (P65), as well as the noncanonical signaling proteins NFKB2 (P52) and RELB, was studied. Ethanol treatment resulted in a significant 73% ± 26% increase of *NFKB1* ($n = 5$; $P < 0.05$; Fig. 2A) and 103% ± 55% upregulation of *RELA* ($n = 5$; $P < 0.05$; Fig. 2B) gene expression. Western blot analysis confirmed NF-κB activation, resulting in significant increases in nuclear RELA protein levels in ethanol- versus control-treated cells ($n = 3$; $P < 0.05$; Fig. 2C, D). No significant changes were observed in *NFKB2* ($n = 3$; $P = 0.21$) or *RELB* ($n = 3$; $P = 0.22$).

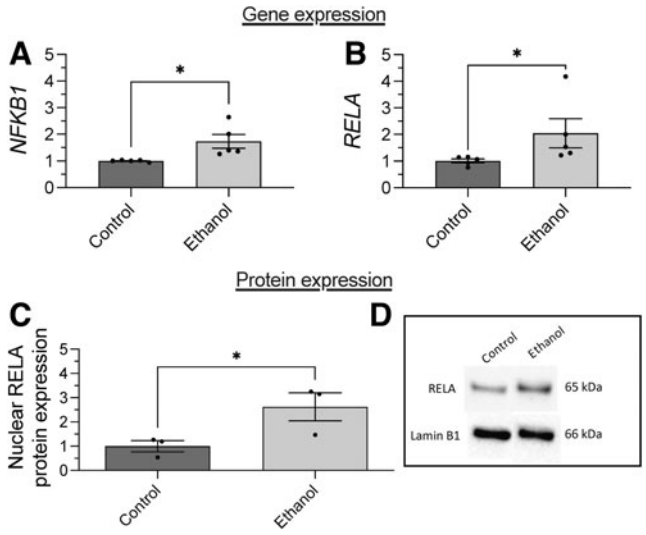

FIG. 2. Gene and protein expression of canonical NF-κB signaling components is increased in ethanol-treated HCE-T. HCE-T were treated with 0.5% ethanol for 6 h, and RNA and protein were extracted for qPCR and western blot analyses, respectively. **(A)** qPCR revealed significant upregulation of (A) *NFKB1* and **(B)** *RELA* in ethanol-treated HCE-T ($n=5$). **(C)** Nuclear protein expression of RELA was also significantly reduced ($n=3$). **(D)** Representative western blot bands for RELA and endogenous nuclear control, Lamin B1. Data are shown as mean ± SEM, with each *circle* representing the mean of a separate experiment. Data were analyzed by Student's *t*-test. $^{*}P<0.05$.

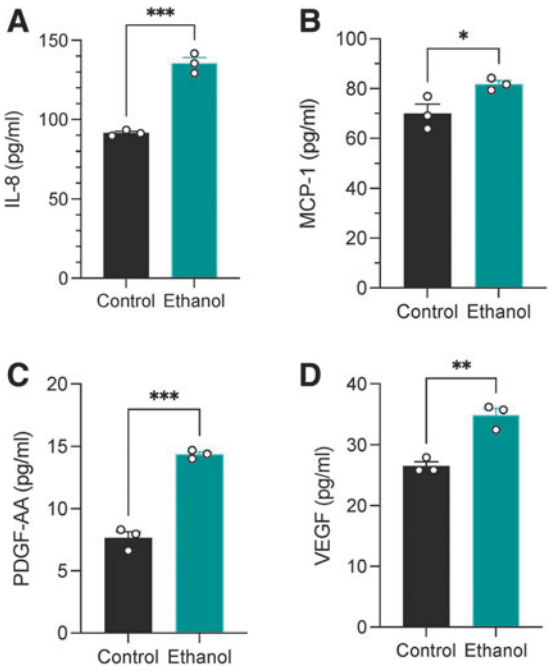

FIG. 3. Secretion of pro-angiogenic cytokines is significantly increased in ethanol-treated HCE-T. Multiplex analysis of cytokine secretion from HCE-T revealed a significant increase in 4 pro-angiogenic cytokines: **(A)** IL-8, **(B)** MCP-1, **(C)** PDGF-AA, and **(D)** VEGF ($n=3$). Data shown as mean ± SEM with each *symbol* representing a separate experiment with duplicate quantification. $^{*}P<0.05$, $^{**}P<0.01$, $^{***}P<0.001$.

Multiplex cytokine analysis revealed significant increases in pro-angiogenic factors in the supernatant from ethanol- versus control-treated cells. Specifically, there was a significant 44 ± 3.7 pg/mL increase of IL-8 ($n=3$, $P=0.001$), 11.8 ± 4 pg/mL increase of MCP-1 ($n=3$, $P=0.05$), 6.7 ± 0.5 pg/mL increase of PDGF-AA ($n=3$, $P=0.001$), and 8.3 ± 1.4 pg/mL increase of VEGF ($n=3$, $P=0.01$) secretion from HCE-T treated with ethanol compared to control (Fig. 3A–D). Interestingly, other well-known pro-inflammatory cytokines, including IL-1, IL-2, IL-6, IL-17, and TNF-α, were not significantly altered or were below the detection threshold Supplementary Table S2.

HCE-T exposed to sublethal ethanol exhibit decreased barrier function and tight junction protein network disorganization

Alcohol is known to elicit deleterious effects on intestinal epithelial tight junction barriers,[23,24] but the effects of alcohol on HCE-T had not previously been studied. HCE-T were stratified as described previously[11] to create multilayered epithelial cells that more closely resemble human corneal physiology. Stratified cells were treated with 0.5% ethanol or left untreated for 4 h. Permeability through the stratified cells was measured using fluorescent permeability standards, specifically the low permeability standard, 6-CF, and the high permeability standard, RhoB (Fig. 4A, B). Ethanol treatment resulted in a significant increase in the apparent permeability index (P_{app}) for both 6-CF (295% ± 130% increase, $P<0.05$, $n=3$–4; Fig. 4C) and RhoB (57.7% ± 7.3% increase, $P<0.05$, $n=3$–4; Fig. 4C).

Similarly, ethanol had pronounced effects on TEER. TEER was measured before (0 h) and after treatments (4 h), and the relative change was calculated. As expected, TEER increased significantly in control cells by 8.9% ± 3.8% (from 232 ± 4 Ω.cm^2 to 253 ± 9 Ω.cm^2; $P<0.05$, $n=4$) as a result of the addition of media to the stratified culture, while ethanol treatment for 4 h reduced TEER by 6.9% ± 1.7% (from 265 ± 9 Ω.cm^2 to 247 ± 4 Ω.cm^2; $P<0.05$; $n=4$).

Epithelial cell barrier properties are primarily contributed by tight junction proteins, including ZO-1 and occludin. Physical forces and chemical changes can lead to barrier breakdown that can manifest as reduction of tight junction protein expression or disorganization of the tight junction barriers. Ethanol treatment resulted in a significant decrease in tight junction organization, TiJOR ($P<0.05$; $n=3$; Fig. 4E) for ZO-1, with a concomitant reduction in ZO-1 immunoreactivity ($P<0.05$; $n=3$; Fig. 4F). Similar changes were observed for occludin TiJOR ($P<0.05$; $n=3$; Fig. 4G) and immunoreactivity ($P<0.05$; $n=3$; Fig. 4H).

Mice consuming alcohol ad libitum *exhibit significant ocular surface pathology*

To test the effect of chronic alcohol consumption, mice were provided *ad libitum* access to the Lieber–DeCarli diet containing 5% alcohol or isocaloric control diet for 10 days, as described previously.[16] Mice were acclimated to the liquid diet without alcohol for a period of 5 days and subsequently randomized into control and alcohol groups. This experimental paradigm (depicted in Fig. 5A) results in significantly increased serum aspartate and alanine

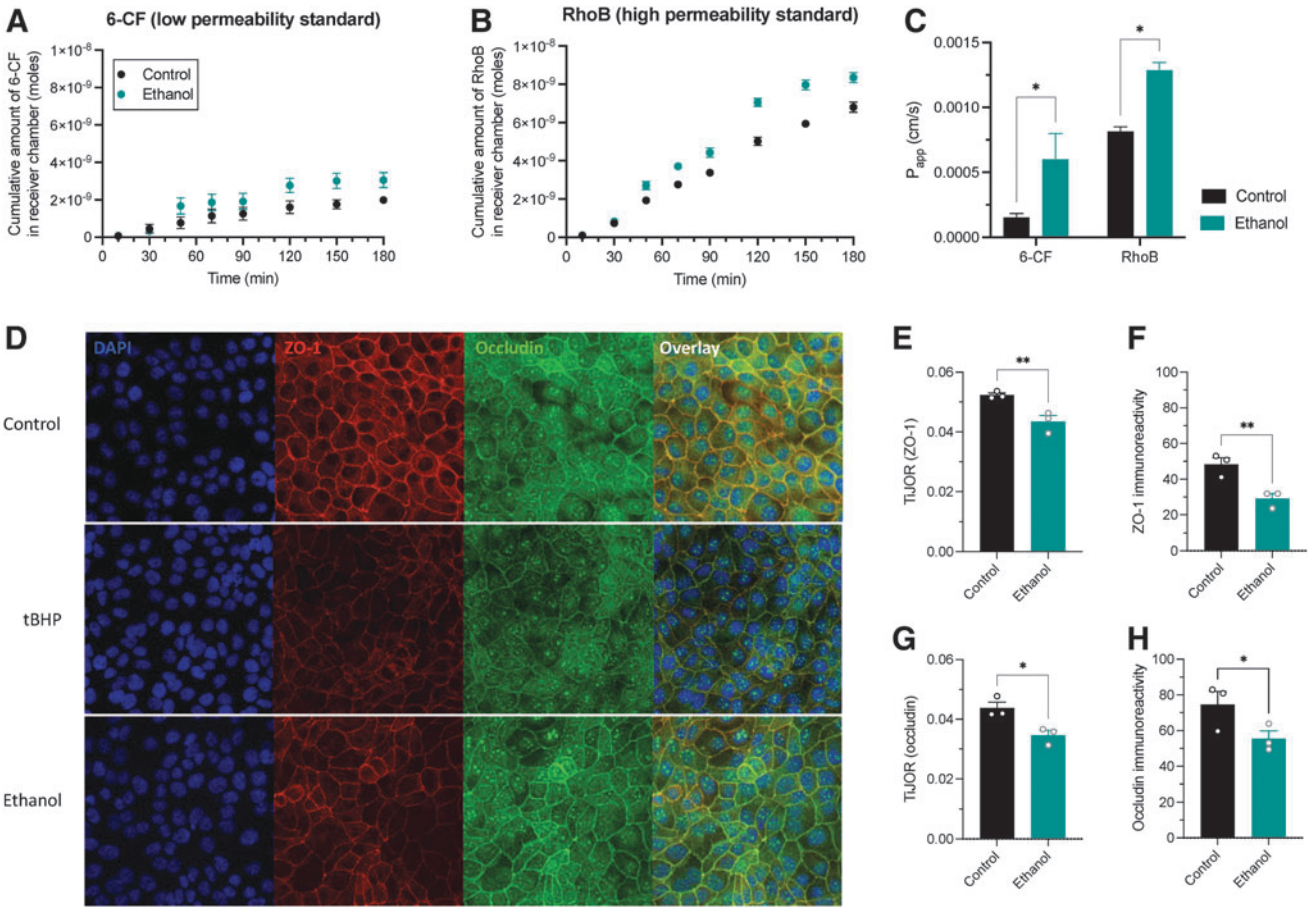

FIG. 4. Ethanol exposure causes barrier dysfunction due to tight junction protein network disorganization in HCE-T. **(A–C)** Stratified HCE-T in transwells were treated with 0.5% ethanol for 4 h, then permeability through the cells and TEER were measured. **(A)** The cumulative amount of low permeability standard, 6-CF, in the receiver chamber over time was increased in ethanol-treated cells compared to control. **(B)** Similarly, the cumulative amount of high permeability standard, RhoB, in the receiver chamber increased significantly over time in ethanol-treated cells compared to control. Data were analyzed by nonparametric Mann–Whitney test. **(C)** The apparent permeability of 6-CF and RhoB through stratified HCE-T was significantly higher in ethanol-treated cells ($n = 3$). **(D)** Representative images of ZO-1 and occludin immunostaining in control and ethanol-treated HCE-T. **(E)** The TiJOR for ZO-1 was significantly disrupted in ethanol-treated cells compared to control ($n = 3$). **(F)** ZO-1 immunoreactivity was significantly lower in ethanol-treated cells, further indicative of disorganization of tight junctions ($n = 3$). **(G)** Similarly, occludin TiJOR was significantly decreased ($n = 3$). **(H)** Occludin immunoreactivity was significantly lower compared with control cells, further supporting the deleterious effect of ethanol on tight junction organization. Data are shown as mean ± SEM from 3 biological replicates, each derived from quantification of five images. Statistical significance was assessed by Student's *t*-test. $*P < 0.05$, $**P < 0.01$. 6-CF, 6-carboxyfluorescein; RhoB, rhodamine B; TEER, transepithelial electrical resistance; TiJOR, tight junction organization rate.

transaminase levels and blood alcohol concentrations of around 160 mg/dL (data not shown[16]).

Overall liquid diet intake was similar between alcohol and control diet groups (2-way ANOVA, $P = 0.46$; Supplementary Fig. S1A), despite some fluctuations throughout the study period (Supplementary Fig. S1B). Similarly, there were no significant changes in body weight (Supplementary Fig. S1C).

Eyes of mice exposed to the Lieber–DeCarli diet were examined by a veterinary ophthalmologist and evaluated using the SPOTS system.[25] No anterior or posterior segment pathology was identified.

Ocular surface pathology was assessed by quantification of tear volumes and corneal fluorescein staining. Tear volumes were not significantly affected by alcohol (Fig. 5B) and increased similarly in both control- and alcohol-fed mice. In contrast, corneal fluorescein staining was significantly higher in alcohol-treated animals, which showed a 151% ± 31% in staining intensity (Fig. 5C). This increase is readily apparent on representative images obtained using a fluorescent microscope and confocal imaging using a Heidelberg Spectralis (Fig. 5D).

Corneal messenger RNA expression of endogenous antioxidant enzymes and NF-κB signaling components is decreased in alcohol-consuming mice

Contrary to the upregulation of genes observed with acute ethanol treatments *in vitro*, gene expression of several antioxidant enzymes in the cornea was lower in alcohol-treated mice compared with control liquid diet-treated mice. Interestingly, *Nrf2* gene expression (*Nfe2l2*) levels were not

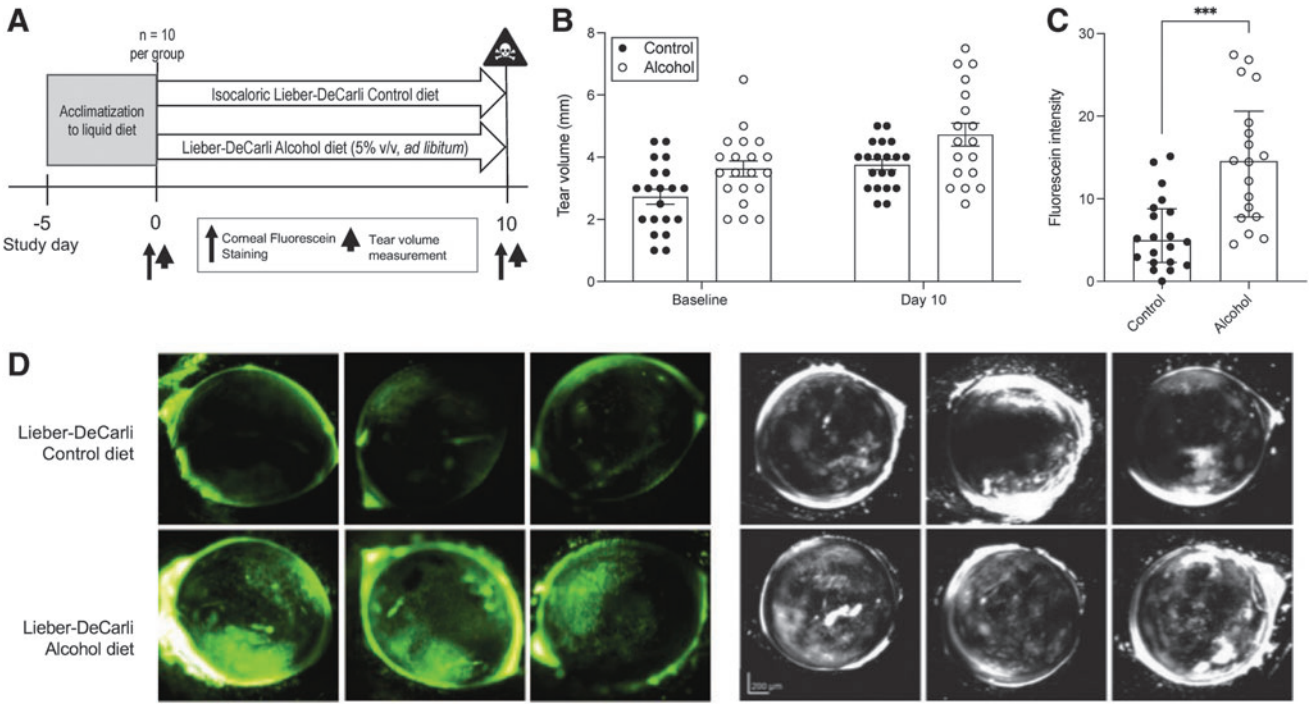

FIG. 5. Alcohol consumption elicits ocular surface damage *in vivo*. **(A)** Graphical depiction of the experimental design. Mice were acclimated to the Lieber–DeCarli liquid diet for 5 days, before receiving either alcohol (5% vol/vol) or control isocaloric ($n = 10$ mice per group). Tear volumes were measured at baseline (0 day) and 10 days. Corneal fluorescein was measured at 10 days, then mice were euthanized for downstream tissue collection, histopathological assessment, and molecular analyses. **(B)** Tear volumes were not significantly affected by alcohol and increased similarly in both control- and alcohol-fed mice. Data were analyzed by 2-way mixed effects analysis ($P < 0.001$ for experimental group, $P < 0.001$ for time, $P = 0.86$ for interaction between the variables), followed by Holm-Šídák multiple comparisons test. **(C)** Intensity of corneal fluorescein staining on the cornea increased significantly in alcohol-fed mice compared with control mice ($P < 0.001$, $n = 18$–20). Data are presented as mean ± SEM with individual data points representing the measurement from a single eye. Data were analyzed by Student's *t*-test. **(D)** Representative images of corneal fluorescein staining from 3 different animals per group acquired using an epifluorescent microscope (*left*) or Heidelberg Spectralis® (*right*). Images show significantly more severe corneal fluorescein staining in alcohol- versus control liquid diet-fed animals. ***$P < 0.001$.

significantly altered (Fig. 6A); however, *Ho-1* and *Cat* levels were significantly decreased by 61% ± 19% ($P < 0.05$, $n = 4$) and 51% ± 4% ($P < 0.05$, $n = 4$), respectively (Fig. 6B, C). Similarly, gene expression of ROS-generating enzymes *Nox1*, *Nox2*, and *Nox4* was decreased by 48% ± 13% ($P < 0.01$; $n = 4$), 72% ± 20% ($P < 0.05$; $n = 4$), and 49% ± 10% ($P < 0.01$; $n = 4$), respectively (Fig. 6E–G). *Nox3* was not expressed in mouse corneas (data not shown). No changes in *Sod* enzyme gene expression were observed (*Sod1*: $P = 0.09$, $n = 4$, Fig. 6D; *Sod2*: $P = 0.34$, $n = 4$, Fig. 6H). Altogether, these data may suggest that chronic moderate alcohol consumption leads to suppression of the endogenous antioxidant response.

Significant reduction of gene expression of *Rela* (by 26% ± 11%, $P < 0.05$, $n = 8$; Fig. 6J) and *Relb* (by 39% ± 8%, $P < 0.001$, $n = 8$; Fig. 6L) was detected in alcohol-consuming mice compared to control. In contrast, *Nfkb1* ($P = 0.31$, $n = 8$, Fig. 6I) and *Nfkb2* ($P = 0.12$, $n = 8$; Fig. 6K) gene expression was similar between groups.

Alcohol induces corneal thinning and oxidative stress in the lacrimal gland, but no immune cell infiltration

Histopathological analysis of cornea and intraorbital and extraorbital lacrimal gland was performed. Total corneal thickness was significantly reduced by 48 ± 20 μm in the alcohol versus control group (Table 1), which could be attributed primarily to a significant 42 ± 15 μm reduction in stromal thickness. Epithelial thickness and number of epithelial cells in the epithelial cell layer were lower, but the difference did not reach statistical significance (Table 1). Histopathological analysis of lacrimal glands did not reveal differences in immune cell infiltration or damage to the lacrimal gland parenchyma, and both intraorbital (Fig. 7A) and extraorbital (Fig. 7B) lacrimal gland were histopathologically normal. However, qPCR revealed a significant 28% ± 9% increase in *Sod1* ($P < 0.05$; $n = 4$; Fig. 7C) and significant 69% ± 13% ($P < 0.01$; $n = 3$–4; Fig. 7C) and 40% ± 9% ($P < 0.01$; $n = 4$; Fig. 7C) decreases in *Sod2* and *Nox1* gene expression, respectively, in the lacrimal glands of alcohol consuming mice versus control. These data suggest that alcohol elicits subclinical oxidative stress-mediated changes in the lacrimal gland.

Discussion

The data herein provide the first experimental evidence that alcohol consumption causes direct damage to the cornea and tissues of the ocular surface through generation of ROS. Our findings support clinical studies that have shown ocular surface signs after acute alcohol consumption and align with

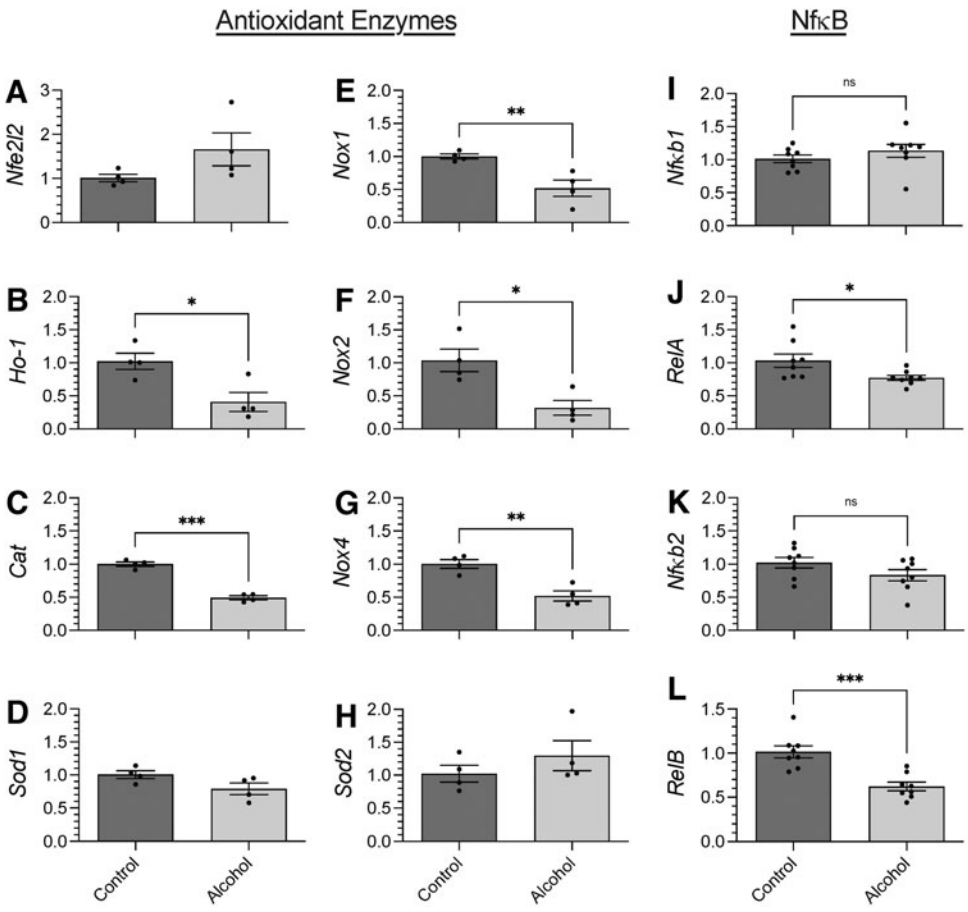

FIG. 6. Corneal expression of several antioxidant and *Nf-κB* genes was significantly decreased in alcohol-receiving mice. Gene expression of the following redox ($n=4$ per group) and NF-κB ($n=8$ per group) signaling proteins was quantified by qPCR from the corneas of control- and alcohol-fed mice: **(A)** *Nfe2l*, **(B)** *Ho-1*, **(C)** *Cat*, **(D)** *Sod1*, **(E)** *Nox1*, **(F)** *Nox2*, **(G)** *Nox4*, **(H)** *Sod2*, **(I)** *Nfkb1*, **(J)** *RelA*, **(K)** *Nfkb2*, **(L)** *RelB*. Data are shown as mean ± SEM, with each data point derived from a single cornea measured in triplicates. Data were analyzed by Student's *t*-test. $^{*}P<0.05$, $^{**}P<0.01$, $^{***}P<0.001$.

epidemiological data that have identified an association between alcohol consumption and the prevalence of DED. As both DED and alcohol use disorder remain underdiagnosed and undertreated in the clinical setting, our data warrant further research into a possible association between alcohol-induced ocular surface signs and the development of DED.

This study used HCE-T for cellular assays, as they are widely used for drug discovery, especially due to their ability to form stratified epithelia that mimic the properties of the corneal epithelium *in vivo*.[8,11,20,26] This makes HCE-T a useful model, for permeability studies; furthermore, we have previously shown that HCE-T possess a potent antioxidant system that responds strongly to exogenous oxidative insults. Despite the utility of cell lines, their proliferative nature does not allow for the testing of chronic alcohol exposure *in vitro*; furthermore, responses may differ from those observed in primary cells.

Table 1. Corneal Thickness Is Reduced in Mice Consuming Alcohol-Containing Liquid Diet

	Total corneal thickness (μm)	*Stromal thickness (μm)*	*Epithelial thickness (μm)*	*No. epithelial cell layers (#)*
Control	123 ± 14	100 ± 11	24 ± 3	4
Alcohol	74 ± 15	58 ± 10	18 ± 5	3
P	0.04[a]	0.02[a]	0.33 (ns)	0.16 (ns)

Histopathological analysis of hematoxylin-eosin (H&E-stained) cornea sections was performed to quantify total corneal thickness, stromal thickness, epithelial thickness, and number of epithelial cell layers. Thickness data are shown as mean ± SEM and were analyzed by Student's *t*-test, while data for the number of epithelial cell layers are shown as median and were analyzed using nonparametric Mann–Whitney test.

[a]$P<0.05$, $n=6$–7 per group.

ns, Not significant; SEM, standard error of the mean.

Our data support the hypothesis that alcohol elicits significant increases of cellular oxidative stress even after exposure to sublethal doses of ethanol for short time periods (4–6 h). This timeline aligns with the reported effects of a single dose of alcohol resulting in significant ocular surface signs 12 h after consumption.[4] Furthermore, the 6 h timepoint was selected to exclude possible confounding effects of cellular proliferation on results. While HCE-T appear relatively resistant to ethanol insult, with only doses of >5% showing reduced cell viability and proliferation, as little as 0.05% v/v ethanol resulted in a statistically significant increase in ROS as quantified by DCF fluorescence, activation of the master regulator of the endogenous antioxidant system, NRF2 (encoded by the *NFE2L2* gene), and an ensuing increase in the expression of downstream genes, including CAT, HO-1, and SOD. These data confirm our previous findings that HCE-T maintain a strong endogenous antioxidant system characteristic of corneal epithelial cells,[8] but notably provide the first published evidence that clinically-relevant sublethal doses of ethanol result in a disbalance between ROS generation and antioxidant response in corneal epithelial cells.

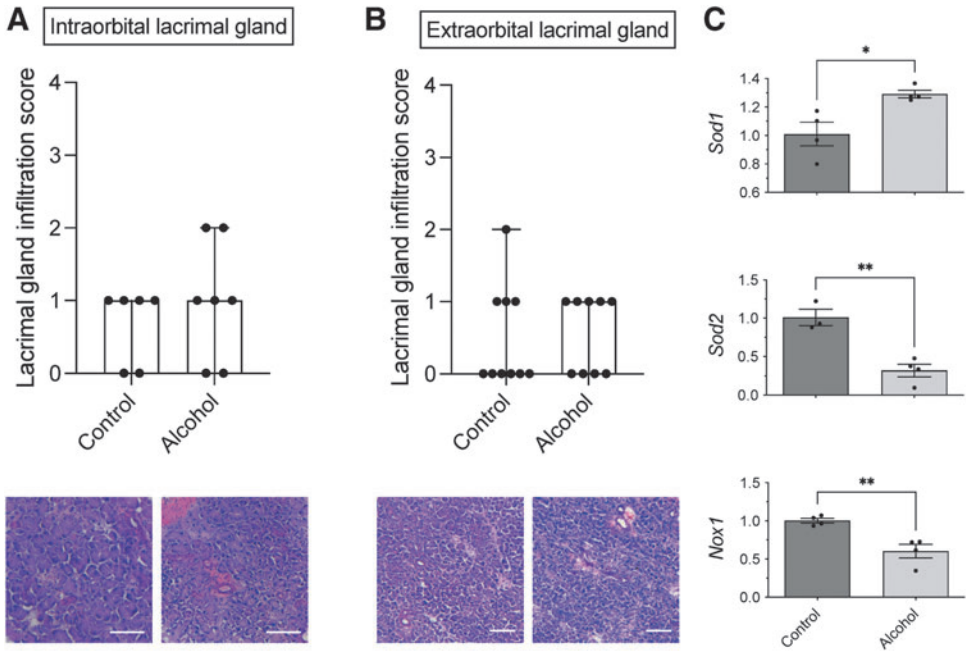

FIG. 7. Lack of histopathological abnormalities, but dysregulation of antioxidant gene expression is suggestive of oxidative stress in the lacrimal gland. **(A)** Intraorbital lacrimal glands were histopathologically normal, without presence of immune cell infiltration ($n=6$ animals). **(B)** Similarly, no abnormalities were identified in extraorbital lacrimal glands ($n=9$–10 animals). Data are shown as median ± interquartile range and were analyzed by Mann–Whitney test. Representative images from control- and alcohol-fed animals are shown. **(C)** qPCR analysis revealed a significant upregulation of *Sod1* gene expression and significant reductions of *Sod2* and *Nox1* in the extraorbital lacrimal glands of alcohol versus control animals ($n=4$ animals). Data are shown as mean ± SEM and were analyzed by Student's *t*-test. $*P<0.05$, $**P<0.01$.

The class of NOX enzymes generates ROS from molecular oxygen. Under physiological conditions, members of the endogenous antioxidant system, such as SOD, create an equilibrium that prevents excess buildup of ROS. Pathological insults cause this balance to be disrupted, leading to dangerously high cellular levels of oxidative stress. Exposure of HCE-T to the acute effects of ethanol resulted in a significant reduction of *NOX3* expression, while *NOX2* expression remained similar. NOX4 is a constitutively expressed member of the NOX family and generally considered an oxygen sensor.[27] Interestingly, HCE-T did not express detectable levels of *NOX4*. In contrast, NOX4 is expressed in the mammalian cornea[28] and it is likely that lack of constitutive expression of *NOX4* may be an artifact of the HCE-T line. In fact, transformed cells do acquire a less differentiated phenotype, which may result in different properties compared with primary cells. In addition, the presence of some genomic abnormalities has been reported for HCE-T,[29] which should be considered when translating *in vitro* findings.

The transcription factor, NFκB, is a key mediator of inflammation, as well as pro- and anti-oxidant gene expression (for review, see Lingappan[30]), and has been implicated as key regulator in ocular surface disease (for review, see Lan et al.[31]). In HCE-T, acute ethanol treatments resulted in the activation of canonical NFκB signaling, resulting in increased gene expression of both *NFkB1* and *RELA*, as well as nuclear translocation of RelA. These data highlight the ability of ethanol to elicit pathological cascades in corneal epithelial cells.

Analysis of cytokines released from HCE-T identified increases in secretion of several proteins associated with corneal injury and neovascularization, including IL-8, MCP-1, VEGF, and PDGF. IL-8 and MCP-1 are key mediators of pathological corneal neovascularization.[32–34] Interestingly, high levels of IL-8 and MCP-1 were found in human corneas with chronic inflammation,[35] and increased levels of MCP-1 were present in the tears of patients with DED,[36] while IL-8 was identified as biomarker for Sjögren's Syndrome dry eye versus non-Sjögren's Syndrome dry eye.[37] HCE-T exposed to desiccating stress or TNFα showed a similar upregulation of IL-8 and MCP-1 as reported herein following the exposure to ethanol.

Mechanistic studies in immortalized corneal epithelial cells have shown that IL-8 release can occur following NF-κB-mediated positive feedback of JNK1/2 phosphorylation after TRPV1 activation.[38] Similarly, application of mitomycin C to corneal fibroblasts in culture resulted in the MAP kinase cascade-mediated upregulation of both IL-8 and MCP-1,[39] while stimulation of NK-1 receptors by substance P in primary HCE-T resulted in IL-8 synthesis through stabilization of chemokine transcripts.[40]

A recent study showed that targeting PDGF-BB resulted in significantly attenuated corneal neovascularization following alkali injury,[41] while the prototypic mediator of neovascularization, VEGF, has also been linked to corneal neovascularization.[42]

Intriguingly, these *in vitro* data support *in vivo* findings that binge alcohol administration to rats[43] resulted in edema and corneal neovascularization (unpublished observations).

Blood alcohol levels in this modified Majchrowicz model are significantly higher (>350 mg/dL[43]) than in animals exposed to the Lieber–DeCarli diet with 5% w/v alcohol (~180 mg/dL; this study[16]) and similar to the amount of ethanol used for the acute *in vitro* studies presented herein. Future studies will investigate the mechanisms of alcohol-induced corneal neovascularization, which is beyond the scope of this article.

Our data on the effects of physiologically-relevant ethanol concentrations on the ocular surface extend previous results by others that have investigated the consequences of toxic ethanol exposure (20%) on corneal epithelial cells and found induction of apoptosis in as little as 20 s.[44] In our studies, we did not find evidence for activation of pro-apoptotic caspases, specifically caspase-3 and caspase-9, following exposure of HCE-T to sublethal concentrations of EtOH (data not shown). Notably, concentrations in excess of 10% EtOH resulted in complete loss of cell viability of HCE-T after 48 h exposure.

One mechanism contributing inflammation and pathological changes of the ocular surface is breakdown of the corneal barrier. The experiments presented herein demonstrate that even short exposure (4 h) to 0.5% ethanol can result in significant disruption of tight junction-mediated corneal barrier. We selected the 4 h timepoint and the 0.5% alcohol concentration to assess effects on barrier function at lowest concentration of ethanol eliciting a significant increase in ROS (Fig. 1C) and at the earliest time of Nrf2 activation (Fig. 1D).

Barrier disruption was evident by an increased permeability index, reduced TEER values, and disruption of organization of tight junction proteins, occludin and ZO-1. The impairment of barrier function was greater than that observed for sublethal doses of oxidative stress or benzalkonium chloride.[20,45] Benzalkonium chloride is still a widely used preservative in ophthalmic formulations, which has been linked to pharmaceutically-induced DED.[46] In preclinical models, repeated benzalkonium chloride instillations are used to induce chronic ocular surface disease,[47,48] which may suggest that chronic exposure to even much lower ethanol may elicit similarly severe chronic ocular surface irritation and inflammation.

Indeed, self-administered systemic exposure for 10 days to low levels of alcohol resulted in a significant increase in corneal fluorescein staining (both intensity and score) in pigmented C57BL/6JRj mice. While chronic alcohol administration can result in dehydration, it is highly unlikely that the observed ocular phenotypes result from dehydration. Body weights of the animals decreased similarly (by <5%) in both control and alcohol diet-fed animals, which can be attributed to the switch from a solid to a liquid diet. Notably, tear volumes slightly increased in both control and alcohol diet-fed animals, suggesting improved hydration as a result of the liquid diet. Furthermore, no effect of the alcohol liquid diet was observed on skin turgor, as part of the routine health evaluation of animals on study.

The Lieber–DeCarli ethanol diet resulted in significant corneal fluorescein staining that was similar in severity to the effect observed following exposure to the DSS model.[8,11,18] This effect was quantified using the widely used modified Oxford-score, as well as by quantifying fluorescein intensity. In addition, alcohol consumption resulted in significantly reduced total corneal thickness (Table 1). It should be noted that hematoxylin-eosin (H&E) staining was performed on cryosections, which is suboptimal for quantification of corneal thickness due to the possible confounding effects of tissue processing artifacts. However, values for total corneal thickness in the control group match *in vivo* pachymetry measurements,[49] as well as values reported for corneas prepared by semithin sectioning.[50] Furthermore, it is likely that artifacts would result in an overestimation of stromal thickness due to separation of the stromal lamellae.

Based on clinical evidence and the *in vitro* results presented herein, it is likely that alcohol administration causes elevated levels of cellular oxidative stress in the tissues of the ocular surface, manifesting as corneal inflammation. While corneal barrier disruption is a well-recognized sign of DED, the alcohol-induced reduction in stromal thickness is not typically associated with DED. Future studies must evaluate whether subacute alcohol-induced corneal toxicity can cause typical signs of DED after long-term chronic exposure.

Gene expression analysis in the cornea of alcohol-treated mice showed an overall reduced expression of antioxidant genes, as well as *Rela* and *Relb*, likely attributed to compensatory changes following prolonged exposure of increased cellular levels of oxidative stress. These findings are partially recapitulated in the lacrimal gland of ethanol-treated mice.

It has previously been shown that mitochondrial oxidative stress in the lacrimal gland can induce lacrimal dysfunction leading to dry disease in rodents. Specifically, deletion of the mev-1 gene resulted in increased ROS levels in the lacrimal gland that manifested as reduced tear volumes, increased corneal fluorescein staining, and infiltration of immune cells into the lacrimal gland.[51,52] While the histopathological evaluation of extraorbital and intraorbital lacrimal glands in this study did not reveal any abnormalities, we observed a decrease in *Nox1*, a significant increase in cytosolic *Sod1*, and a concomitant decrease in mitochondrial *Sod2* in extraorbital lacrimal glands. These changes are consistent with an adaptive change to the ROS/antioxidant balance inside the mitochondria following prolonged exposure to alcohol.

Interestingly, in intestinal epithelial cells decreased *Nox1* expression was associated with antioxidative effects, including reduction in LDH release and increases in SOD activity.[53] Furthermore, disruption of the redox balance can promote the nuclear translocation of SOD1 to act as a *bona fide* transcription factor for antioxidant and cell repair genes.[54] As such, the observed reduction in *Sod2* gene expression may be a compensatory change following prolonged tissue exposure to oxidative stress.

Differential effects on SOD isoform expression by ethanol were also detected in corneal epithelial cells exposed to the acute effects of ethanol *in vitro* versus in corneal tissue from prolonged (10 days) exposure to an alcohol-containing diet *in vivo*. Expression of cytosolic SOD1 is typically associated with activation of the endogenous antioxidant system and associated with antioxidative effects. SOD1 expression is also regulated by stress-response gene-encoded regulator of calcineurin 1 (RCAN1).[55]

Intriguingly, while transient increases in RCAN1 exert anti-inflammatory effects, chronic overexpression and/or upregulation is associated with deleterious pro-oxidative changes and chronic diseases, including Alzheimer's

disease.[55] The idea of the differential effects of transient versus chronic stress has also been conceptualized in the notions of oxidative eustress and oxidative distress (for review, see Herb and Schramm[56]). Altogether, the observed gene expression changes suggest that chronic alcohol exposure results in the generation of deleterious levels of oxidative stress in the tissues of the ocular surface, ultimately resulting in manifestation of alcohol-induced DED.

We have previously shown the pharmacologic efficacy of antioxidants in models for ocular surface disease, including the mouse DSS model[8,11] and a rabbit model for irritant-induced dry eye.[57] Furthermore, the cardiolipin peroxidation inhibitor, SkQ1, was approved in Russia for the treatment of dry eye and is currently being tested in Phase 3 clinical trials in the United States.[58] Given the involvement of redox dyshomeostasis in alcohol-induced ocular surface pathology, antioxidants may be effective in preventing and/or reversing the effects of alcohol.

Future studies will assess the effects of alcohol consumption in other ocular tissues, investigate possible sex differences, and test the ability of antioxidants and anti-inflammatory drugs in attenuating or preventing alcohol-induced ocular surface disease.

Conclusion

Our data suggest that alcohol exposure causes increased levels of oxidative stress in the tissues of the ocular surface, especially the cornea, resulting in corneal toxicity in mice. To our knowledge, this is the first systematic investigation of the effects of alcohol on ocular surface pathology in rodents. Our results align with population-based findings that have linked past alcohol consumption to a greater incidence of DED, as well as clinical studies that have demonstrated the acute effects of alcohol on the ocular surface. Future studies are needed to elucidate the possible association between alcohol-induced corneal toxicity and dry-eye disease.

Acknowledgments

The authors thank all members of the Alcohol Research Program at Loyola University Chicago, Health Sciences Division for their support and guidance for this project. This article is based, in part, on research performed as part of Anita Ghosh's doctoral thesis (located at https://www.proquest.com/docview/2671974260).

Authors' Contributions

Conceptualization, A.K.G., S.K.; methodology, A.K.G., S.R., S.K.; formal analysis, A.K.G., S.I., S.K.; investigation, A.K.G., R.C., D.N., A.Z., S.I., J.M.E., S.R., S.K.; data curation, A.K.G., S.K.; writing—original draft preparation, A.K.G., S.K.; writing—review and editing, A.K.G., R.C., D.N., A.Z., S.I., J.M.E., S.R., S.K.; supervision, S.R. and S.K.; project administration, A.K.G., S.K.; funding acquisition, A.K.G., S.K. All authors have read and agreed to the published version of the article.

Author Disclosure Statement

A.K.G., R.C., D.N., A.Z., S.R. are employees of Experimentica Ltd., a preclinical contract research organization; S.R. and S.K. hold equity ownership in Experimentica Ltd.; A.K.G. serves as Officers of the Board for Experimentica Ltd. A.K.G. and S.K. are inventors on a filed patent application on drug targets for DED assigned to eyeNOS, Inc., unrelated to this article. A.K.G. holds equity ownership in eyeNOS, Inc., S.K. holds equity ownership in K&P Scientific, LLC. A.K.G. serves as a consultant for K&P Scientific, LLC. S.K. conducts academic research in areas of interest similar to the business interests of Experimentica Ltd. and K&P Scientific, LLC. The terms of this arrangement have been reviewed and approved by Loyola University Chicago in accordance with its conflict-of-interest policy. The funders had no role in the design of the study; in the collection, analyses, or interpretation of data; in the writing of the article; or in the decision to publish the results. S.I. and J.M.E. declare no financial conflicts of interest.

Funding Information

This work was supported by the National Institutes of Health (grant Nos. AA013527, EY032440); the Illinois Society for the Prevention of Blindness; Fight for Sight; the Richard A. Perritt M.D. Charitable Foundation; the Dr. John P. and Therese E. Mulcahy Endowed Professorship in Ophthalmology (Loyola University Chicago); K&P Scientific, LLC; and Experimentica Ltd.

Supplementary Material

Supplementary Figure S1
Supplementary Table S1
Supplementary Table S2

References

1. Craig JP, Nichols KK, Akpek EK, et al. TFOS DEWS II definition and classification report. Ocul Surf 2017;15:276–283.
2. Moss SE, Klein R, Klein BE. Prevalence of and risk factors for dry eye syndrome. Arch Ophthalmol 2000;118:1264–1268.
3. Cumurcu T, Gunduz A, Cumurcu BE, et al. The changes in tear film parameters and impression cytology in heavily drinking men. Cornea 2013;32:237–241.
4. Kim JH, Kim JH, Nam WH, et al. Oral alcohol administration disturbs tear film and ocular surface. Ophthalmology 2012;119:965–971.
5. Das SK, Vasudevan DM. Alcohol-induced oxidative stress. Life Sci 2007;81:177–187.
6. Tsermpini EE, Plemenitas Iljes A, Dolzan V. Alcohol-induced oxidative stress and the role of antioxidants in alcohol use disorder: A systematic review. Antioxidants (Basel) 2022;11:1374.
7. Araki K, Ohashi Y, Sasabe T, et al. Immortalization of rabbit corneal epithelial cells by a recombinant SV40-adenovirus vector. Invest Ophthalmol Vis Sci 1993;34:2665–2671.
8. Ghosh AK, Thapa R, Hariani HN, et al. Poly(lactic-co-glycolic acid) nanoparticles encapsulating the prenylated flavonoid, xanthohumol, protect corneal epithelial cells from dry eye disease-associated oxidative stress. Pharmaceutics 2021;13:1362.
9. Kaja S, Payne AJ, Naumchuk Y, et al. Plate reader-based cell viability assays for glioprotection using primary rat optic nerve head astrocytes. Exp Eye Res 2015;138:159–166.

10. Maciulaitiene R, Pakuliene G, Kaja S, et al. Glioprotection of retinal astrocytes after intravitreal administration of memantine in the mouse optic nerve crush model. Med Sci Monit 2017;23:1173–1179.
11. Ziniauskaite A, Ragauskas S, Ghosh AK, et al. Manganese(III) tetrakis(1-methyl-4-pyridyl) porphyrin, a superoxide dismutase mimetic, reduces disease severity in in vitro and in vivo models for dry-eye disease. Ocul Surf 2019;17:257–264.
12. Kaja S, Hilgenberg JD, Rybalchenko V, et al. Polycystin-2 expression and function in adult mouse lacrimal acinar cells. Invest Ophthalmol Vis Sci 2011;52:5605–5611.
13. Kaja S, Duncan RS, Longoria S, et al. Novel mechanism of increased Ca^{2+} release following oxidative stress in neuronal cells involves type 2 inositol-1,4,5-trisphosphate receptors. Neuroscience 2011;175:281–291.
14. Schindelin J, Arganda-Carreras I, Frise E, et al. Fiji: An open-source platform for biological-image analysis. Nat Methods 2012;9:676–682.
15. Terryn C, Sellami M, Fichel C, et al. Rapid method of quantification of tight-junction organization using image analysis. Cytometry A 2013;83:235–241.
16. Bertola A, Mathews S, Ki SH, et al. Mouse model of chronic and binge ethanol feeding (the NIAAA model). Nat Protoc 2013;8:627–637.
17. Lin Z, Liu X, Zhou T, et al. A mouse dry eye model induced by topical administration of benzalkonium chloride. Mol Vis 2011;17:257–264.
18. Ziniauskaite A, Ragauskas S, Hakkarainen JJ, et al. Efficacy of trabodenoson in a mouse keratoconjunctivitis sicca (KCS) model for dry-eye syndrome. Invest Ophthalmol Vis Sci 2018;59:3088–3093.
19. Livak KJ, Schmittgen TD. Analysis of relative gene expression data using real-time quantitative PCR and the 2(-Delta Delta C(T)) Method. Methods 2001;25:402–408.
20. Hakkarainen JJ, Reinisalo M, Ragauskas S, et al. Acute cytotoxic effects of marketed ophthalmic formulations on human corneal epithelial cells. Int J Pharm 2016;511: 73–78.
21. Faul F, Erdfelder E, Lang AG, et al. G*Power 3: A flexible statistical power analysis program for the social, behavioral, and biomedical sciences. Behav Res Methods 2007; 39:175–191.
22. Faul F, Erdfelder E, Buchner A, et al. Statistical power analyses using G*Power 3.1: Tests for correlation and regression analyses. Behav Res Methods 2009;41:1149–1160.
23. Wood S, Pithadia R, Rehman T, et al. Chronic alcohol exposure renders epithelial cells vulnerable to bacterial infection. PLoS One 2013;8:e54646.
24. Ma TY, Nguyen D, Bui V, et al. Ethanol modulation of intestinal epithelial tight junction barrier. Am J Physiol 1999;276:G965–G974.
25. Eaton JS, Miller PE, Bentley E, et al. The SPOTS system: An ocular scoring system optimized for use in modern preclinical drug development and toxicology. J Ocul Pharmacol Ther 2017;33:718–734.
26. Becker U, Ehrhardt C, Schneider M, et al. A comparative evaluation of corneal epithelial cell cultures for assessing ocular permeability. Altern Lab Anim 2008;36:33–44.
27. Nisimoto Y, Diebold BA, Cosentino-Gomes D, et al. Nox4: A hydrogen peroxide-generating oxygen sensor. Biochemistry 2014;53:5111–5120.
28. Hakami NY, Dusting GJ, Chan EC, et al. Wound healing after alkali burn injury of the cornea involves Nox4-type NADPH oxidase. Invest Ophthalmol Vis Sci 2020;61:20.
29. Yamasaki K, Kawasaki S, Young RD, et al. Genomic aberrations and cellular heterogeneity in SV40-immortalized human corneal epithelial cells. Invest Ophthalmol Vis Sci 2009;50:604–613.
30. Lingappan K. NF-kappaB in oxidative stress. Curr Opin Toxicol 2018;7:81–86.
31. Lan W, Petznick A, Heryati S, et al. Nuclear factor-kappaB: Central regulator in ocular surface inflammation and diseases. Ocul Surf 2012;10:137–148.
32. Strieter RM, Kunkel SL, Elner VM, et al. Interleukin-8. A corneal factor that induces neovascularization. Am J Pathol 1992;141:1279–1284.
33. Yoshida S, Yoshida A, Matsui H, et al. Involvement of macrophage chemotactic protein-1 and interleukin-1beta during inflammatory but not basic fibroblast growth factor-dependent neovascularization in the mouse cornea. Lab Invest 2003;83:927–938.
34. Usui T, Sugisaki K, Iriyama A, et al. Inhibition of corneal neovascularization by blocking the angiotensin II type 1 receptor. Invest Ophthalmol Vis Sci 2008;49:4370–4376.
35. Spandau UH, Toksoy A, Verhaart S, et al. High expression of chemokines Gro-alpha (CXCL-1), IL-8 (CXCL-8), and MCP-1 (CCL-2) in inflamed human corneas in vivo. Arch Ophthalmol 2003;121:825–831.
36. Na KS, Mok JW, Kim JY, et al. Correlations between tear cytokines, chemokines, and soluble receptors and clinical severity of dry eye disease. Invest Ophthalmol Vis Sci 2012;53:5443–5450.
37. Akpek EK, Wu HY, Karakus S, et al. Differential diagnosis of Sjogren versus non-Sjogren dry eye through tear film biomarkers. Cornea 2020;39:991–997.
38. Wang Z, Yang Y, Yang H, et al. NF-kappaB feedback control of JNK1 activation modulates TRPV1-induced increases in IL-6 and IL-8 release by human corneal epithelial cells. Mol Vis 2011;17:3137–3146.
39. Chou SF, Chang SW, Chuang JL. Mitomycin C upregulates IL-8 and MCP-1 chemokine expression via mitogen-activated protein kinases in corneal fibroblasts. Invest Ophthalmol Vis Sci 2007;48:2009–2016.
40. Tran MT, Lausch RN, Oakes JE. Substance P differentially stimulates IL-8 synthesis in human corneal epithelial cells. Invest Ophthalmol Vis Sci 2000;41:3871–3877.
41. Chen L, Wu H, Ren C, et al. Inhibition of PDGF-BB reduces alkali-induced corneal neovascularization in mice. Mol Med Rep 2021;23:238.
42. Philipp W, Speicher L, Humpel C. Expression of vascular endothelial growth factor and its receptors in inflamed and vascularized human corneas. Invest Ophthalmol Vis Sci 2000;41:2514–2522.
43. Kouzoukas DE, Schreiber JA, Tajuddin NF, et al. PARP inhibition in vivo blocks alcohol-induced brain neurodegeneration and neuroinflammatory cytosolic phospholipase A2 elevations. Neurochem Int 2019;129:104497.
44. Chen CC, Chang JH, Lee JB, et al. Human corneal epithelial cell viability and morphology after dilute alcohol exposure. Invest Ophthalmol Vis Sci 2002;43: 2593–2602.
45. Droy-Lefaix MT, Bueno L, Caron P, et al. Ocular inflammation and corneal permeability alteration by benzalkonium chloride in rats: A protective effect of a myosin light chain kinase inhibitor. Invest Ophthalmol Vis Sci 2013;54: 2705–2710.
46. Goldstein MH, Silva FQ, Blender N, et al. Ocular benzalkonium chloride exposure: Problems and solutions. Eye (Lond) 2022;36(2):361–368.

47. Xiong C, Chen D, Liu J, et al. A rabbit dry eye model induced by topical medication of a preservative benzalkonium chloride. Invest Ophthalmol Vis Sci 2008;49:1850–1856.
48. Carpena-Torres C, Pintor J, Perez de Lara MJ, et al. Optimization of a rabbit dry eye model induced by topical instillation of benzalkonium chloride. J Ophthalmol 2020; 2020:7204951.
49. Schulz D, Iliev ME, Frueh BE, et al. In vivo pachymetry in normal eyes of rats, mice and rabbits with the optical low coherence reflectometer. Vision Res 2003;43:723–728.
50. Henriksson JT, McDermott AM, Bergmanson JP. Dimensions and morphology of the cornea in three strains of mice. Invest Ophthalmol Vis Sci 2009;50:3648–3654.
51. Uchino Y, Kawakita T, Ishii T, et al. A new mouse model of dry eye disease: Oxidative stress affects functional decline in the lacrimal gland. Cornea 2012;31(Suppl 1):S63–S67.
52. Uchino Y, Kawakita T, Miyazawa M, et al. Oxidative stress induced inflammation initiates functional decline of tear production. PLoS One 2012;7:e45805.
53. Li H, He Y, Zhang C, et al. NOX1 down-regulation attenuated the autophagy and oxidative damage in pig intestinal epithelial cell following transcriptome analysis of transport stress. Gene 2020;763:145071.
54. Tsang CK, Liu Y, Thomas J, et al. Superoxide dismutase 1 acts as a nuclear transcription factor to regulate oxidative stress resistance. Nat Commun 2014;5:3446.
55. Ermak G, Cheadle C, Becker KG, et al. DSCR1(Adapt78) modulates expression of SOD1. FASEB J 2004;18:62–69.
56. Herb M, Schramm M. Functions of ROS in macrophages and antimicrobial immunity. Antioxidants (Basel) 2021;10:313.
57. Ghosh AK, Bacellar-Galdino M, Iqbal S, et al. Topical porphyrin antioxidant protects against ocular surface pathology in a novel rabbit model for particulate matter-induced dry eye disease. J Ocul Pharmacol Ther 2022; 38(4):294–304.
58. Brzheskiy VV, Efimova EL, Vorontsova TN, et al. Results of a multicenter, randomized, double-masked, placebo-controlled clinical study of the efficacy and safety of visomitin eye drops in patients with dry eye syndrome. Adv Ther 2015;32:1263–1279.

Received: December 31, 2022
Accepted: March 19, 2023

Address correspondence to:
Dr. Simon Kaja
Loyola University Chicago
Ocular Pharmacology and Drug Discovery Laboratory
Center for Translational Research and Education
2160 South First Avenue
Maywood, IL 60153
USA

E-mail: skaja@luc.edu